Functional MRI of Human Brain Activation Combining High Spatial and Temporal Resolution by a CINE FLASH Technique

Klaus-Dietmar Merboldt, Gunnar Krüger, Wolfgang Hänicke, Andreas Kleinschmidt, Jens Frahm

Functional mapping of human brain activation has been accomplished at high spatial *and* temporal resolution (voxel size 4.9 μl, temporal increment 100 ms). The approach was based on oxygenation-sensitive long-echo time FLASH MRI sequences synchronized to multiply repeated cycles of visual stimulation in a CINE acquisition mode. This high temporal resolution revealed that stimulus-related signal intensity changes in human visual cortex display an initial latency followed by increases extending over several seconds. Furthermore, the temporal characteristics of the complete CINE MRI signal time course depended on the absolute and relative durations of activation and control periods and, for example, caused an apparent absence of a poststimulation "undershoot" phenomenon. Complementing hyperoxygenation due to rapid hemodynamic adjustments, these results suggest signal intensity modulation by enhanced oxygen consumption and concomitant deoxygenation during prolonged and/or repetitive stimulation.

Key words: brain, function; brain, activation; magnetic resonance, functional; visual cortex.

INTRODUCTION

Magnetic resonance imaging (MRI) shows considerable potential for mapping the functional anatomy of the human brain (e.g., see ref. 1). While initial studies (2) required the application of an exogenous contrast agent to identify activation-related increases in cerebral blood volume, more recent and preferable techniques focus on experimental conditions that allow attributing MRI signal changes to alterations of cerebral blood oxygenation (CBO) mediated via the endogenous contrast properties of paramagnetic deoxyhemoglobin (3, 4). In fact, simultaneous recording of CBO by gradient-echo MRI and near infrared spectroscopy clearly established a decrease of deoxyhemoglobin concentration during activation as a common source of "functional contrast" in either technique (5).

The purpose of the present study was to develop a method that allows CBO-sensitive MRI at high temporal resolution while retaining high spatial resolution as the most intriguing feature (6). In addition to technical feasibility of the chosen strategy, this approach should support a deepened understanding of temporal signal characteristics and their dependence on protocol timing. Although echo-planar imaging (EPI) is able to acquire CBO-sensitive MR images within less than 100 ms (7, 8), successive repetitions of FID-based EPI sequences would suffer from limited spatial resolution due to the single-shot requirement in conjunction with a T_2*-limited acquisition window. The method presented here attempts to combine long-echo time FLASH sequences (4, 6) with a CINE acquisition mode in analogy to that used for functional MRI of the cardiovascular system (9). It allows recording of brain MRI signal changes at a temporal resolution corresponding to the repetition time *TR*, i.e., tens of milliseconds.

The principle of data acquisition is shown in Fig. 1 for a protocol comprising visual stimulation (activation) and darkness (control). During each stimulation cycle the same Fourier line is acquired (constant phase-encoding gradient) every repetition interval *TR*. Related Fourier lines during *n* repetitive cycles are based on incremented phase-encoding gradients that cover the phase-encoding direction of *k*-space by *n* samples. A total of *N* images which span the duration of a single stimulation cycle (i.e., a period of $N \times TR$) is then reconstructed from reordered data. Access to high temporal resolution in this "quasi-realtime" MRI experiment is at the expense of prolonging the overall acquisition time to about 1 h, e.g., when using 128 phase-encodings and a 30-s stimulation cycle. A preliminary account of this work (10) and a related report where CINE MRI has been applied *after the end* of a visual stimulus have appeared in abstract form (11).

METHODS

CBO-Sensitive CINE MRI

All studies were conducted at 2.0 T (Siemens Magnetom SP4000) with use of the standard imaging headcoil. For CBO-sensitive CINE MRI the chosen stimulus cycle was synchronized to an RF-spoiled long-echo time FLASH sequence with a temporal resolution of $TR = 100$ ms, an echo time of $TE = 30$ ms, and a flip angle of $\alpha = 20°$. The choice of *TE* represents a compromise between oxygenation sensitivity due to T_2* contrast, image signal-to-noise, and unwanted contributions from motion and macroscopic susceptibility differences (6). To ensure that the observed signal changes were entirely due to changes in CBO rather than blood flow velocity, the flip angle was even further reduced to 10° in some experiments. Intraview motion correction was achieved by using first-order

MRM 34:639–644 (1995)

From the Biomedizinische NMR Forschungs GmbH, Max-Planck-Institut für Biophysikalische Chemie, Göttingen, Germany.

Address correspondence to: Jens Frahm, Ph.D., Biomedizinische NMR Forschungs GmbH, Max-Planck-Institut für Biophysikalische Chemie, Postfach 2841, D-37018 Göttingen, Germany.

Received October 20, 1994; revised April 11, 1995; accepted June 9, 1995.

0740-3194/95 $3.00

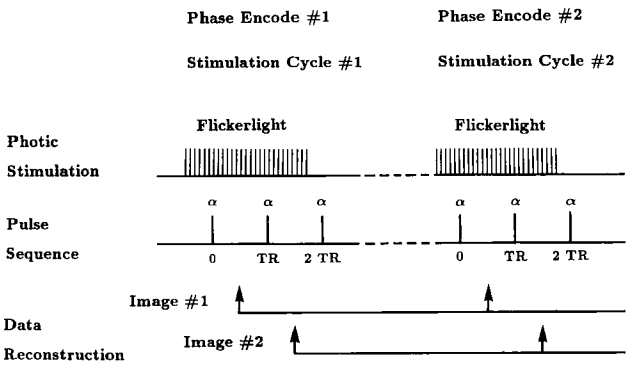

FIG. 1. Schematic outline of the CINE acquisition mode used for functional mapping of brain activation at high spatial and temporal resolution. Data acquisition of the low flip angle gradient-echo sequence (flip angle α) is synchronized to the stimulation cycle. Because during each cycle the same Fourier line is measured, n-fold repetitions of the stimulation cycle are required with incremented phase-encoding gradients. The process results in a set of 2D image raw data with a temporal resolution of TR.

gradient-moment nulling in the frequency-encoding and slice selection axes. The spatial resolution was either 4.9 or 9.8 μl corresponding to data matrices of 64 × 256 or 128 × 256 covering a 200-mm field-of-view (FOV) with a slice thickness of 4 mm.

A total of 15 functional neuroimaging examinations of young healthy volunteers were performed. Written informed consent was obtained from all subjects before the investigations. The volunteers wore ear plugs and had their heads positioned in a vacuum cap. The measuring cabin was kept dark during the investigation. For visual stimulation a pattern of red flickerlights (10 Hz) was projected binocularly via fiber optics.

Before time-resolved CINE MRI the optimum imaging section was determined by T_1-weighted 3D MRI (RF-spoiled FLASH, TR/TE = 18/7.5 ms, flip angle 20°, matrix 32 × 256 × 256, FOV 200 mm, partition thickness 4 mm), flow-sensitized anatomic MRI (RF-spoiled FLASH, TR/TE = 70.3/7.5 ms, flip angle 60°, matrix 256 × 256, FOV 200 mm, slice thickness 4 mm), and functional mapping of calcarine cortex with a conventional CBO-sensitive imaging protocol (RF-spoiled FLASH, TR/TE = 63/30 ms, α = 10°) at a temporal resolution of 6 s (4, 6,

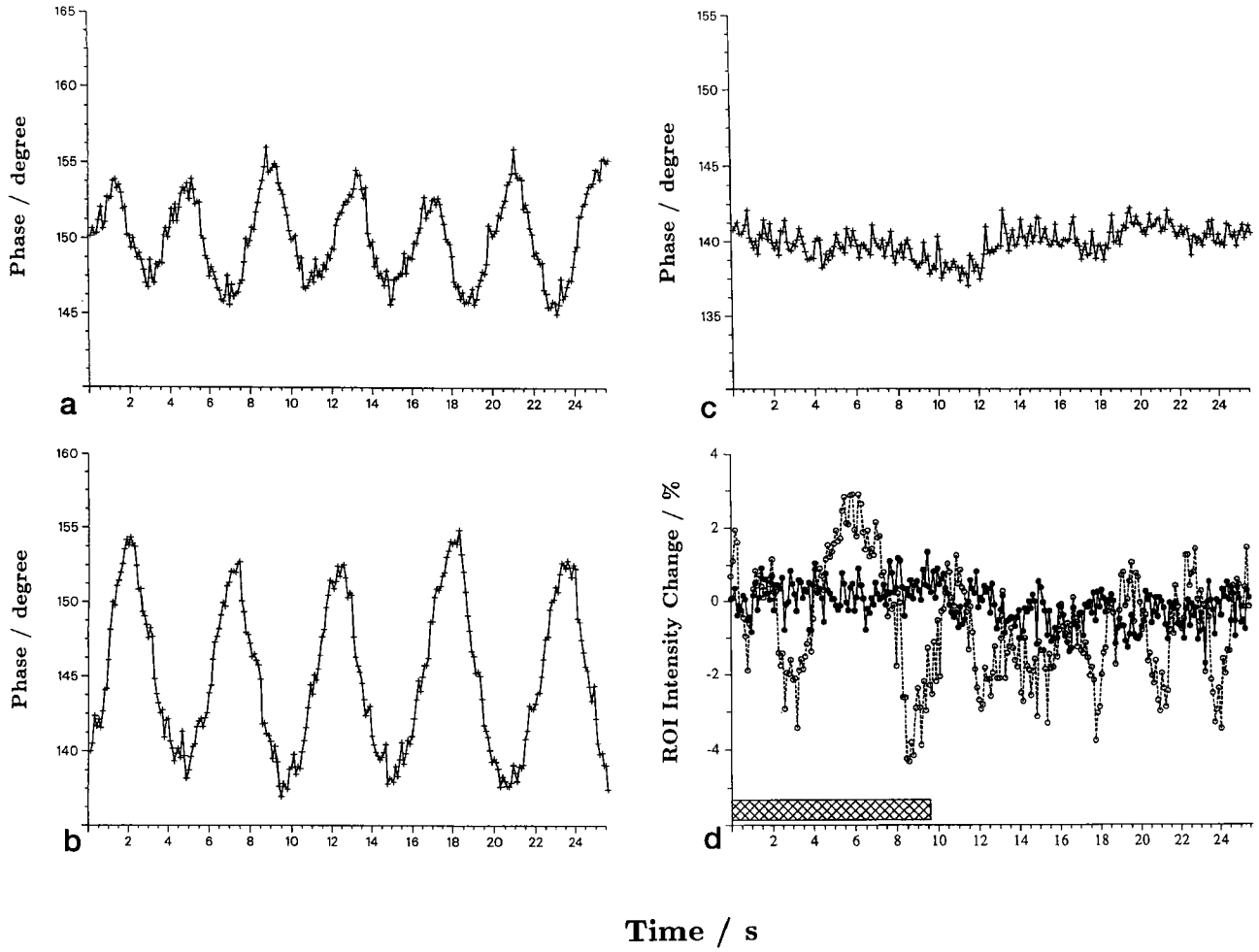

FIG. 2. The influence of respiration on the phase of a low flip angle gradient-echo signal (TR/TE = 100/30 ms, flip angle 20°) during (a) normal breathing, (b) deep breathing, and (c) breath-holding calculated at the echo maximum, respectively. (d) ROI intensity fluctuations during visual stimulation in frontal gray matter (control region C in Fig. 3c) in CINE FLASH MR images without (open circles) and with phase correction (solid circles) as described in text.

12). The latter technique was also used for investigations of the dynamic physiologic approach to steady-state conditions for either one long period of persistent stimulation or a rapid succession of multiple short cycles of stimulation. For CINE studies, synchronization of stimulation and data acquisition was accomplished by a home-built gate driven by trigger pulses from the MRI pulse sequence. Duration of activation and reference periods could be adjusted by separate counters and varied from 0.5 to 30 s for visual stimulation and from 16.0 to 44.8 s for darkness.

Correction of Motion-Induced Phase Errors

Although careful positioning and fixation suppress subject motion to some extent, phase errors still occur mainly due to respiratory motion (13). Figure 2 shows the phase of the gradient-echo signal without phase-encoding (TR/TE = 100/30 ms, α = 20°) as a function of time during normal breathing, deep breathing, and breath-holding. If uncorrected as depicted in Fig. 2d (open circles), such phase variations may result in MRI signal intensity changes of several percent that superimpose onto stimulus-related signal alterations.

To account for these unavoidable though largely periodic phase errors, a strategy was developed in accordance with the phase analysis of linear motion by Korin *et al.* (14). Phase values θ_r from the complex raw data of a reference image selected for minimal motion artifact were taken to replace corresponding phases θ_i of all other image raw data. The procedure represents a complex multiplication of the MRI signal with $e^{i(\theta_r - \theta_i)}$ and corrects for inter-view motion. The second trace in Fig. 2d (solid circles) illustrates the marked reduction in signal fluctuation resulting from improved phase stability. The region-of-interest (ROI) used was located in nonactivated frontal gray matter (region C in Fig. 3c).

RESULTS AND DISCUSSION

A visual stimulation study is summarized in Fig. 3 showing the section chosen, a flow-sensitized anatomic image in this plane, and a corresponding CBO-sensitive image reconstructed from a phase-corrected CINE FLASH MRI experiment. In accordance with the desired emphasis on deoxyhemoglobin-related signal contrast, potential contributions from changes in flow velocity were minimized by the acquisition of images emphasizing T_2* sensitivity (TR/TE = 100/30 ms, α = 20°). The difference map in Fig. 3d was obtained by subtracting the average of 20 baseline images (darkness) from a corresponding average of images during activation. This map was nearly identical to an activation map obtained by a non-CINE technique (not shown) confirming that the phase correction scheme did not affect the topographic pattern of stimulus-related CBO changes.

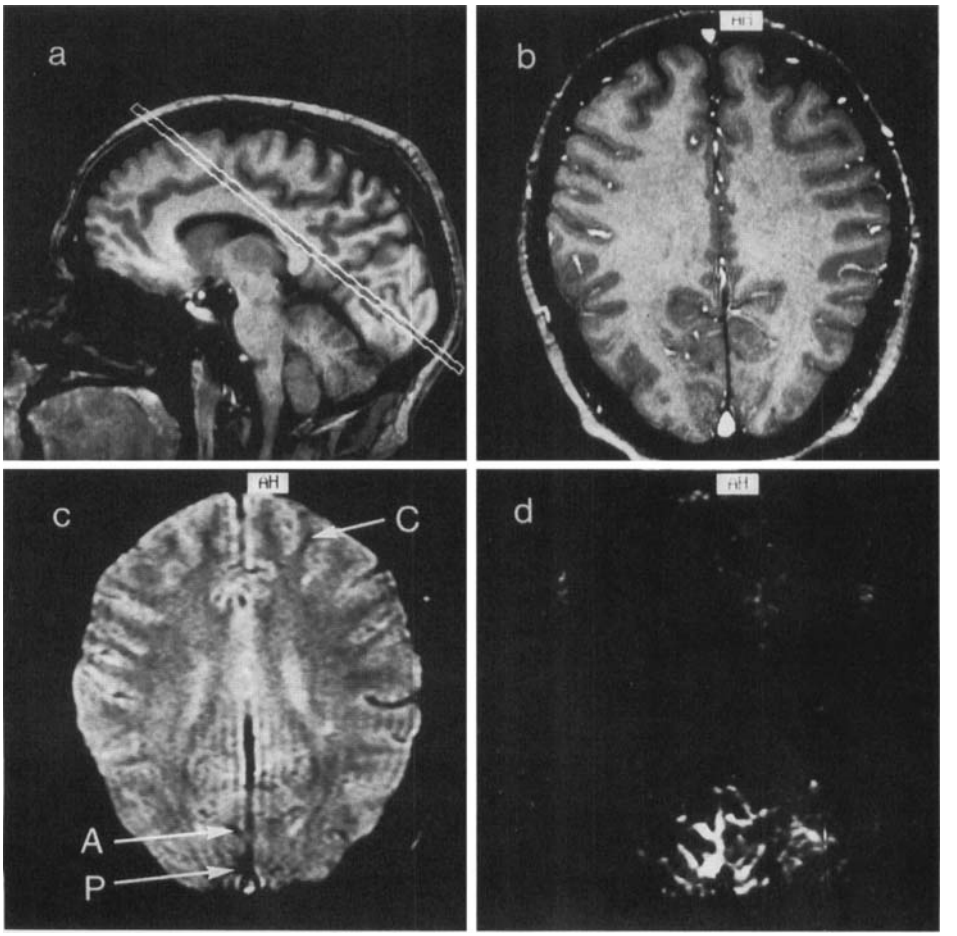

FIG. 3. (a) Plane orientation for activation studies of visual cortex, (b) corresponding flow-sensitized anatomic image, (c) CBO-sensitive image (RF-spoiled FLASH, TR/TE = 100/30 ms, flip angle 20°, matrix 128 × 256, FOV 200 mm, slice thickness 4 mm) from the CINE MRI data set, and (d) CINE MRI difference map obtained by subtracting an averaged baseline image from an averaged image acquired during visual stimulation. The arrows indicate locations of the control (C), anterior (A), and posterior (P) ROIs used in Figs. 2 and 4, respectively.

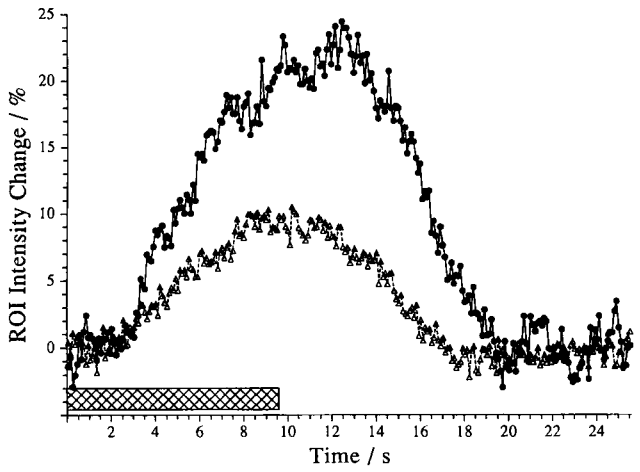

FIG. 4. MRI signal time courses representing activation from a posterior (solid circles) and anterior ROI (open triangles) in calcarine cortex during 9.6 s of visual stimulation followed by 16 s of darkness (same data set as in Fig. 3).

Signal time courses from two ROIs in calcarine cortex (Fig. 4) describe the temporal response pattern as revealed by CINE MRI. The protocol comprised cycles of 9.6 s flickerlight stimulation and 16 s of darkness and yielded peak-to-peak MRI signal intensity changes of up to 25%. Latencies ranging from 2 to 3 s between the onset of stimulation and the first occurrence of MRI signal alterations are in agreement with previous observations (1). No systematic latency differences could be assigned to either distinct cortical areas or tissue compartments (gray matter versus macroscopic vessel). However, detectability of subtle temporal differences may have been hampered by limited and regionally variable contrast-to-noise as well as by residual motion artifact. Future studies aiming at exploiting conceivable latency information are expected to benefit from a further reduction of interview (or inter-image) phase errors by using navigator echoes (13, 15). In general, the present findings underline that stimulus-related MRI signal changes represent neuronal activation only after a timespan required for hemodynamic adjustments that are mediated by slow neurovascular coupling.

The influence of protocol timing on CINE MRI signal time courses is demonstrated in Fig. 5 for stimulation/darkness periods of 30/21.2 s, 18/36 s, 6/45.2 s, and 0.5/25.1 s, respectively. In contrast to activation protocols covering only a single stimulation period, the CINE

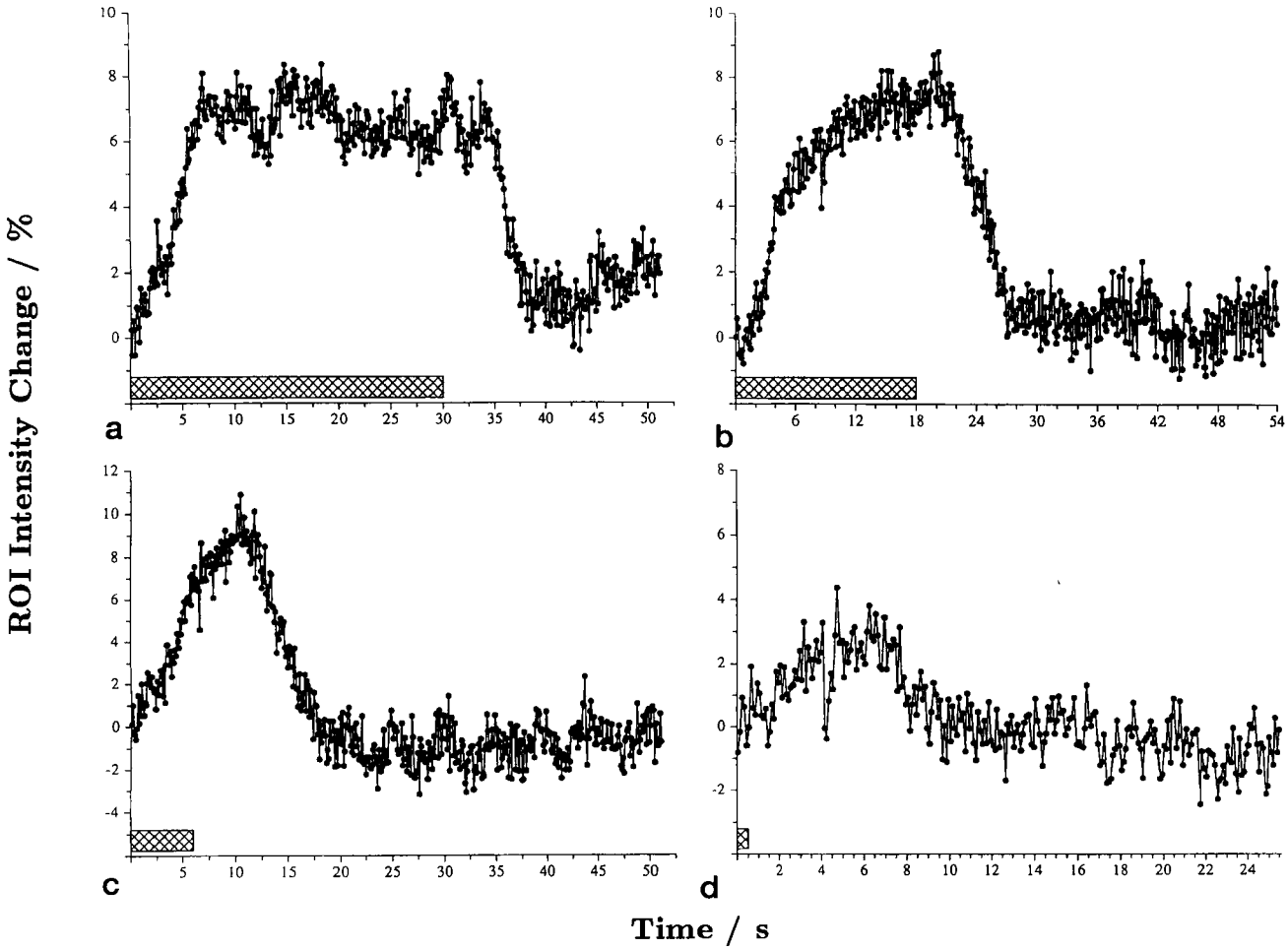

FIG. 5. MRI signal time courses representing activation of visual cortex using visual stimulation/darkness periods of (a) 30 s/21.2 s, (b) 18 s/36 s, (c) 6 s/45.2 s, and (d) 0.5 s/25.1 s. The data originate from one subject different from the one shown in Fig. 4.

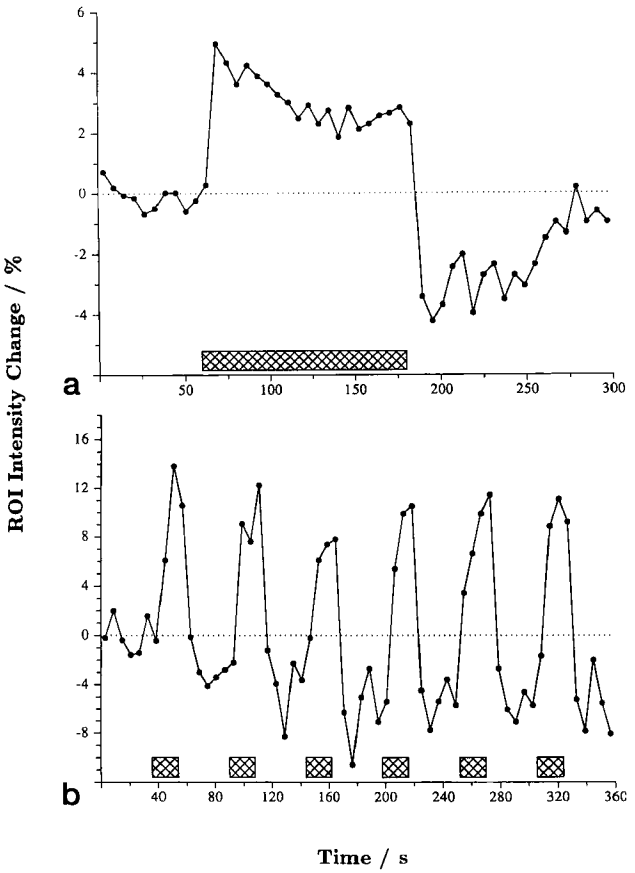

FIG. 6. MRI signal time courses representing activation of visual cortex in the same subject as in Fig. 5 using (a) 120 s of visual stimulation (average of 10 independent acquisitions) and (b) six repetitive cycles of 18 s of visual stimulation and 36 s of darkness. Dotted lines represent basal conditions before the onset of stimulation (sequential RF-spoiled FLASH, *TR/TE* = 62.5/30 ms, flip angle 10°, matrix 96 × 256, rectangular FOV 150 × 200 mm, slice thickness 4 mm).

response patterns reflect the physiologic behavior in an equilibrium state created by multiply repeated cycles of stimulation and rest. During 30 s of stimulation and with a "duty cycle" of 59% (Fig. 5a) the signal intensity exhibits a plateau phase, whereas the 18 s stimulation period with a 33% duty cycle (Fig. 5b) shows a biphasic signal rise with an initial steep increase followed by a slower enhancement (16). Signal increases persisting or not even appearing until after the end of activation were found for 6 or 0.5 s stimulation periods, respectively (Figs. 5c and 5d).

These findings were in qualitative agreement across subjects and regions. They may be explained by the interplay of two counteracting processes that affect oxygenation levels in primary visual cortex in relation to physiologic activation, i.e., *rapid* changes in perfusion and *slow* adjustments of oxidative metabolism. While the initial uncoupling of oxygen delivery and consumption (17) causes a rise in CBO, prolonged neuronal activation leads to an upregulation of oxygen consumption and its recoupling to perfusion after 3–4 min (18). Although detailed modeling of steady-state CBO time courses for the conditions of a CINE MRI experiment would require knowledge of underlying rate constants, the absence of a poststimulation "undershoot" phenomenon (compare Fig. 5) may be a direct consequence of the dynamic equilibrium state reached by repeated stimulations without sufficient recovery intervals. While Fig. 6a demonstrates that the poststimulation return to basal CBO levels requires at least 120 s, Fig. 6b illustrates the cumulative effect of six successive cycles of visual stimulation (18 s) and darkness (36 s) in analogy to the CINE protocol used for Fig. 5b. After about three cycles, the system approaches a deoxygenated basal state relative to the prestimulation CBO level that represents a new steady-state equilibrium most likely at increased oxygen consumption (i.e., deoxyhemoglobin formation). Because the absolute CBO increase after the onset of stimulation remains unaffected in this situation, the CINE MRI signal time course apparently lacks the undershoot effect.

In conclusion, the present study extends previous emphasis on predominance of hemodynamic response characteristics in CBO-sensitive MRI of human brain activation to the secondary influence of altered oxygen metabolism induced by prolonged and/or repetitive stimulation. As a consequence, functional mapping of paradigm-specific brain activation may not only be affected by a large number of MRI physical parameters, but also depends on the modulation of underlying physiologic processes by protocol timings. These observations may help to optimize stimulation paradigms and acquisition schemes for mapping functional brain anatomy by MRI techniques sensitized to changes in blood oxygenation.

REFERENCES

1. Functional MRI of the Brain, Syllabus, Workshop, June 17–19, 1993, Arlington, Virginia, Society of Magnetic Resonance in Medicine, Berkeley, 1993.
2. J. W. Belliveau, D. N. Kennedy, R. C. McKinstry, B. R. Buchbinder, R. Weisskoff, M. S. Cohen, J. M. Vevea, T. J. Brady, B. R. Rosen, Functional mapping of the human visual cortex by magnetic resonance imaging. *Science* **254,** 716–719 (1991).
3. S. Ogawa, T. M. Lee, A. R. Kay, D. W. Tank, Brain magnetic resonance imaging with contrast dependent on blood oxygenation. *Proc. Natl. Acad. Sci. (USA)* **87,** 9868–9872 (1990).
4. J. Frahm, K. D. Merboldt, W. Hänicke, A. Kleinschmidt, H. Boecker, Brain or vein—oxygenation or flow? On signal physiology in functional MRI of human brain activation. *NMR Biomed.* **7,** 45–53 (1994).
5. H. Obrig, A. Kleinschmidt, K. D. Merboldt, U. Dirnagl, J. Frahm, A. Villringer, Monitoring of cerebral blood oxygenation during human brain activation by simultaneous high-resolution MRI and near-infrared spectroscopy, *in* "Proc., SMR, 2nd Annual Meeting, San Francisco, 1994," p. 67.
6. J. Frahm, K. D. Merboldt, W. Hänicke, Functional MRI of human brain activation at high spatial resolution. *Magn. Reson. Med.* **29,** 139–144 (1993).
7. E. A. DeYoe, J. Neitz, P. A. Bandettini, E. C. Wong, J. S. Hyde, Time course of event-related MR signal enhancement in visual and motor cortex, *in* "Proc., SMRM, 11th Annual Meeting, Berlin, 1992," p. 1824.
8. J. W. Belliveau, J. R. Baker, K. K. Kwong, B. R. Rosen, Functional neuroimaging combining fMRI, MEG, and EEG, *in* "Proc., SMRM, 12th Annual Meeting, New York, 1993," p. 6.

9. G. H. Glover, N. J. Pelc, Rapid-gated Cine MRI technique, *in* "Magnetic Resonance Annual" (H. Y. Kressel, Ed.), pp. 299–333, Raven, New York, 1988.
10. K. D. Merboldt, G. Krüger, W. Hänicke, J. Frahm, FLASH MRI of human brain activation using a CINE technique. An approach towards high temporal and spatial resolution, *in* "Proc., SMR, 2nd Annual Meeting, San Francisco, 1994," p. 432.
11. R. Beisteiner, G. Gomiscek, V. Edward, C. Techtmeister, E. Moser, High temporal and spatial resolution in functional imaging on clinical imagers: Investigating blood flow changes in the millisecond range, *in* "Proc., SMR, 2nd Annual Meeting, San Francisco, 1994," p. 661.
12. J. Frahm, K. D. Merboldt, W. Hänicke, The influence of the slice-selection gradient on functional MRI of human brain activation. *J. Magn. Reson. B* **103,** 91–93 (1994).
13. X. Hu, S.-G. Kim, Reduction of signal fluctuation in functional MRI using navigator echoes. *Magn. Reson. Med.* **31,** 495–503 (1994).
14. H. W. Korin, F. Farzaneh, R. C. Wright, S. J. Riederer, Compensation for effects of linear motion in MR imaging. *Magn. Reson. Med.* **12,** 99–113 (1989).
15. R. L. Ehman, J. P. Felmlee, Adaptive technique for high-definition MR imaging of moving structures. *Radiology* **173,** 255–263 (1989).
16. R. S. Menon, X. Hu, P. Andersen, K. Uğurbil, S. Ogawa, Cerebral oxy/deoxy hemoglobin changes during neural activation: MRI time course correlates to optical reflectance measurements, *in* "Proc., SMR, 2nd Annual Meeting, San Francisco, 1994," p. 68.
17. P. T. Fox, M. E. Raichle, Focal physiological uncoupling of cerebral blood flow and oxidative metabolism during somatosensory stimulation in human subjects. *Proc. Natl. Acad. Sci. (USA)* **83,** 1140–1144 (1986).
18. J. Frahm, G. Krüger, K. D. Merboldt, A. Kleinschmidt, Dynamic uncoupling and recoupling of perfusion and oxidative metabolism during focal brain activation in man. *Magn. Reson. Med.*, in press.